Hyperfine Interact (2007) 175:77–84
DOI 10.1007/s10751-008-9591-2

Structural, Mössbauer and magnetic studies on Mn-substituted barium hexaferrites prepared by high energy ball milling

Puneet Sharma · R. A. Rocha · S. N. de Medeiros · A. Paesano Jr · B. Hallouche

Published online: 9 April 2008

Abstract In the present study, $BaFe_{12-X}Mn_XO_{19}$ hexaferrites were prepared by high-energy ball milling and subsequent thermal annealing. The structural and magnetic characterizations were carried out by X-ray diffraction, Mössbauer spectroscopy and magnetization measurements. The analyses showed that manganese occupies all iron sites, decreasing the magnetization and increasing the coercivity.

Keywords Barium hexaferrite · High-energy ball milling · Mössbauer spectroscopy

1 Introduction

Since the discovery of the M-type hexagonal ferrites in 1950s, it has being of great interest due to its application as permanent magnetic materials and perpendicular recording media [1, 2]. The main reason for its great success is its low cost at moderate magnetic properties. Many attempts have been made to improve its magnetic properties by divalent-tetravalent and trivalent cationic substitution for Fe^{3+} ion situated at the five different crystallographic sites, i.e., the octahedral (12k, $4f_2$, 2a), tetrahedral ($4f_1$) and trigonal bipyramidal (2b) sites. The most extensively studied divalent-tetravalent substitutions were Co–Ti [3], Co–Sn [4], Ni–Ti [5], Zn–Ti [6, 7], Zn–Zr [8], whereas some studied trivalent cations are Al, Ga, Cr, Sc and In [9–11]. In addition, some trivalent metal cations that can also exist in divalent and tetravalent state such as manganese, have been investigated. Collomb et al. [12], *e.g.*, carried out a magnetic structure study on manganese substitution, considering its Mn^{2+},

P. Sharma · R. A. Rocha · S. N. de Medeiros · A. Paesano Jr (✉)
Departamento de Física, Universidade Estadual de Maringá, Av. Colombo, 5790, 87.020-900 Maringá, Paraná, Brazil
e-mail: paesano@wnet.com.br

B. Hallouche
Departamento de Química e Física, UNISC, Santa Cruz do Sul, Rio Grande do Sul, Brazil

Mn^{3+} and Mn^{4+} states at the different crystallographic sites. Turrili et al. [13] also investigated Mn^{2+}-Ti^{4+} substitution. Recently, electron energy-loss spectroscopy (EELS) studies on some Mn-ferrites and Mn-substituted barium hexaferrites suggested that manganese remains in Mn^{3+} ionic state [14].

In the present study, Mn-substituted barium hexaferrites were prepared by high-energy ball milling. The influence of Mn^{3+} ion substitution on the structure and magnetic properties was systematically investigated and discussed.

2 Experimental

$BaFe_{12-X}Mn_XO_{19}$ samples with X=0.5, 1.0, 1.5, and 2.0 were prepared by high-energy ball milling for 30 h in free atmosphere, using laboratory grade compounds $BaCO_3$, Fe_2O_3, and Mn_2O_3, in a planetary mill with hardened steel vial and balls. The ball-to-powder ratio was 10:1 and the speed rotation was 300 rpm. Further, the milled powders were annealed at 1050°C for 2 h, also in free atmosphere, using a resistance furnace. The heating and cooling rates were 51°C/min.

The phase characterization of powders was carried out in a SHIMADZU-6000 X-ray diffractometer. The XRD patterns of heat-treated samples were refined by the Rietveld method (Fullprof Suite-2000 software). Mössbauer characterizations were performed at room temperature and 80 K, in the transmission geometry, using a conventional spectrometer operating in a constant acceleration mode. The gamma rays were provided by a $^{57}Co(Rh)$ source. The Mössbauer spectra were analyzed with a non-linear least-square routine, with Lorentzian line shape. The magnetic properties of randomly pressed powders were measured in a vibrating sample magnetometer, with a maximum field of 1.5 T.

3 Results and discussions

The X-ray diffractograms of the non-substituted and X=2.0 substituted barium hexaferrite samples are shown in Fig. 1. Both samples show the barium hexaferrite as a single phase. However, a minor peak of hematite is also observed in the non-substituted sample. No peaks for the Mn_2O_3 phase were observed. Also, the presence of metallic iron was not detected in the diffractograms, which was further confirmed by Mössbauer spectroscopy. Thus, no significant contamination from the milling media is expected.

Figure 2 shows the lattice parameters, a and c, as a function of the Mn content, as obtained by Rietveld analysis. The decrease in the lattice parameter c means that the unit cell shrinks perpendicularly to the basal plane.

Figure 3 shows the Mössbauer spectra for the X=0.0, 1.0, 2.0 samples, taken at room temperature (Fig. 2a) and 80 K (Fig. 2b). They were fitted with five and six discrete sextets, respectively. For the non-substituted sample, the fit was carried out constraining the subspectral areas to the ratio 6:2:2:1:1 for the 12k, $4f_1$, $4f_2$, 2a and 2b sites, respectively. With the purpose of simplification, no component for the hematite phase was considered, due to its minor occurrence. However, for substituted samples the subspectral areas of all five sites were kept free. The fitted parameters were the hyperfine magnetic fields (B_{hf}), the quadrupolar shifts (QS), the isomer shifts (IS) and the line widths (Γ) besides the subspectral areas.

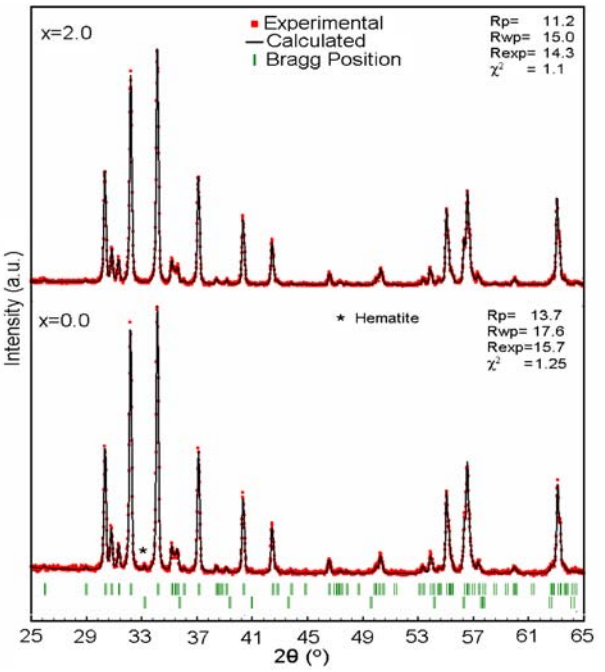

Fig. 1 X-ray diffraction patterns for the $BaFe_{12}O_{19}$ and $BaFe_{10}Mn_2O_{19}$ samples

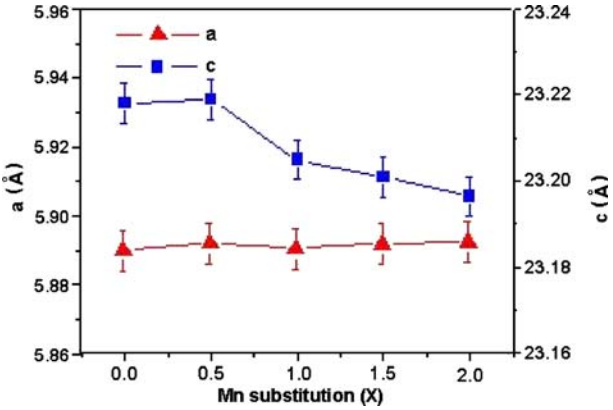

Fig. 2 Variation in the lattice parameter with the Mn content

The fit for the $X \geq 1$ samples measured at RT required six sextets. Because of the IS and QS similarity and after inspecting the relative areas, we concluded that the 12 K was split in two components, henceforth designed as $12k_1$ and $12k_2$. The split may be attributed to different neighborhoods for the iron in the crystallographic site 12k, resultant from the manganese substitution. One of these new components has a hyperfine field weakened relatively to the other, indicating a little smaller magnetic moment for the iron in this specific neighborhood. On the other hand, a small difference between the quadrupolar splittings of the two components can also be verified.

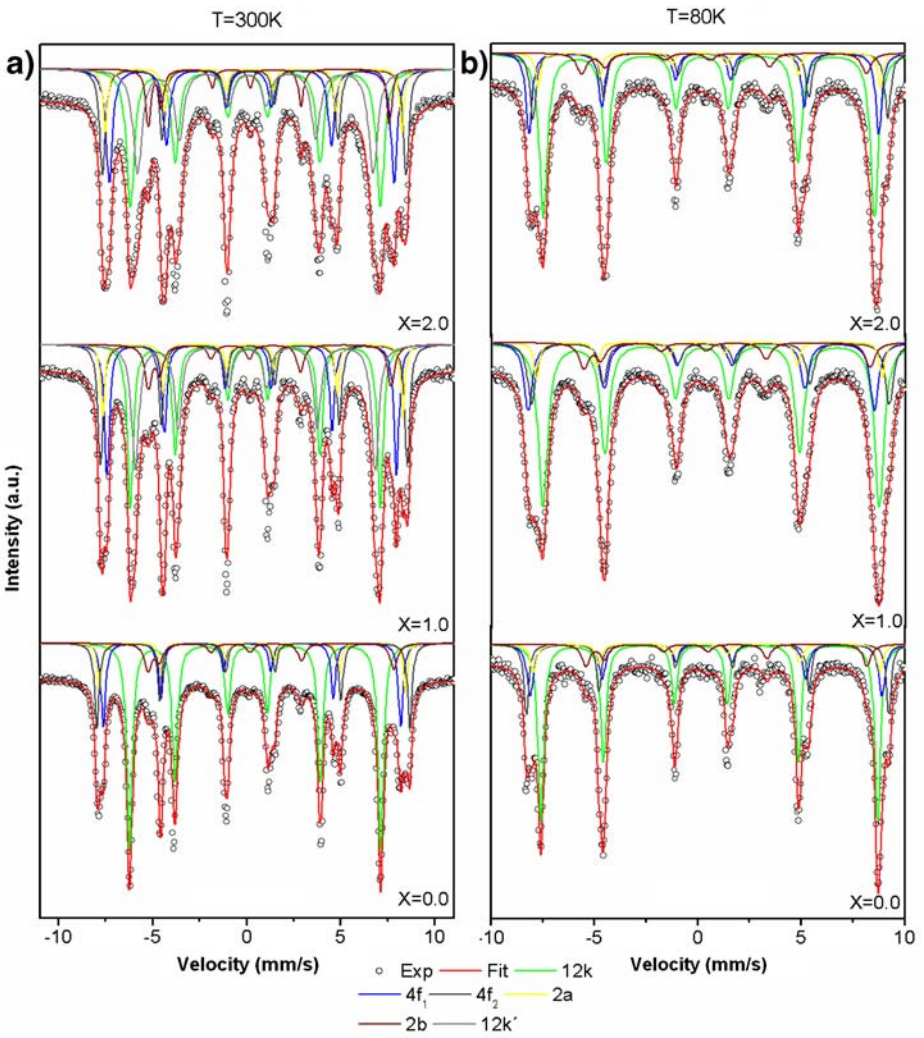

Fig. 3 Mössbauer spectra taken at 300 K (**a**) and 80 K (**b**) for Mn-substituted (X=0.0, 1.0 and 2.0) barium hexaferrites

Interestingly, the split relative to the 12k site disappears as the temperature goes down since, again, five components were enough for the fits. This reveals that both iron magnetic moments are temperature sensible in a diverse manner, though reaching virtually the same value at 80 K. The hyperfine parameters from measurements at 300 K and 80 K are given in Tables 1 and 2, respectively. It can be seen that the B_{hf} values decrease monotonically with the manganese content, including the average values for the 12k's components, revealing the progressive weakening of the magnetic moments of iron at all sites. On the contrary, reducing the temperature, the magnetic hyperfine fields increase up to 20% of their RT values.

Table 1 Hyperfine parameters and subspectral areas for the $BaFe_{12-X}Mn_XO_{19}$ samples measured at 300 K

Mn content (X)	Site	B_{hf} (T)	IS[a] (mm/s)	QS (mm/s)	Γ (mm/s)	S (%)
0.0	12k	41.4	0.24	0.40	0.35	50.0
	$4f_1$	49.0	0.25	0.25	0.29	16.7
	$4f_2$	51.6	0.27	0.16	0.28	16.7
	2a	50.6	0.25	0.09	0.25	8.3
	2b	40.5	0.21	2.15	0.46	8.3
0.5	12k	41.0	0.24	0.40	0.39	50.4
	$4f_1$	48.3	0.16	0.20	0.28	17.2
	$4f_2$	51.1	0.26	0.17	0.26	16.4
	2a	49.9	0.26	0.09	0.24	7.8
	2b	40.2	0.18	2.13	0.45	8.2
1.0	$12k_1$	41.2	0.24	0.41	0.37	25.8
	$12k_2$	39.5	0.25	0.40	0.38	24.5
	$4f_1$	47.7	0.17	0.18	0.32	17.7
	$4f_2$	50.6	0.28	0.19	0.32	16.3
	2a	49.5	0.25	0.13	0.25	7.8
	2b	40.0	0.17	2.10	0.45	7.9
1.5	$12k_1$	41.2	0.24	0.41	0.45	28.2
	$12k_2$	39.2	0.24	0.38	0.44	23.4
	$4f_1$	47.4	0.18	0.17	0.39	18.4
	$4f_2$	50.4	0.28	0.20	0.33	15.8
	2a	49.1	0.27	0.16	0.27	7.0
	2b	40.0	0.17	2.03	0.40	7.2
2.0	$12k_1$	41.2	0.24	0.39	0.50	27.9
	$12k_2$	38.9	0.24	0.39	0.57	23.9
	$4f_1$	47.0	0.19	0.14	0.41	19.0
	$4f_2$	50.1	0.29	0.22	0.35	15.0
	2a	48.9	0.27	0.18	0.26	7.0
	2b	39.7	0.17	2.0	0.44	7.2

[a] Relative to α–Fe

Table 2 Hyperfine parameters and subspectral areas for the X=0.0, 1.0, 2.0 samples measured at 80 K

Mn content (X)	Site	B_{hf} (T)	IS[a] (mm/s)	QS (mm/s)	Γ (mm/s)	S (%)
0.0	12k	50.6	0.35	0.40	0.35	50.0
	$4f_1$	52.9	0.36	0.10	0.40	16.7
	$4f_2$	54.3	0.37	0.23	0.30	16.7
	2a	51.8	0.28	0.24	0.21	8.3
	2b	41.8	0.27	2.20	0.43	8.3
1.0	12k	50.4	0.38	0.42	0.61	50.8
	$4f_1$	51.9	0.20	0.0	0.48	18.5
	$4f_2$	53.6	0.47	0.19	0.42	16.6
	2a	51.8	0.22	0.57	0.22	6.3
	2b	42.9	0.32	2.10	0.55	7.8
2.0	12k	49.6	0.34	0.33	0.74	51.6
	$4f_1$	52.4	0.24	0.0	0.35	18.9
	$4f_2$	53.1	0.48	0.20	0.34	15.3
	2a	51.4	0.28	0.50	0.28	6.9
	2b	42.7	0.35	1.75	0.61	7.3

[a] Relative to α–Fe

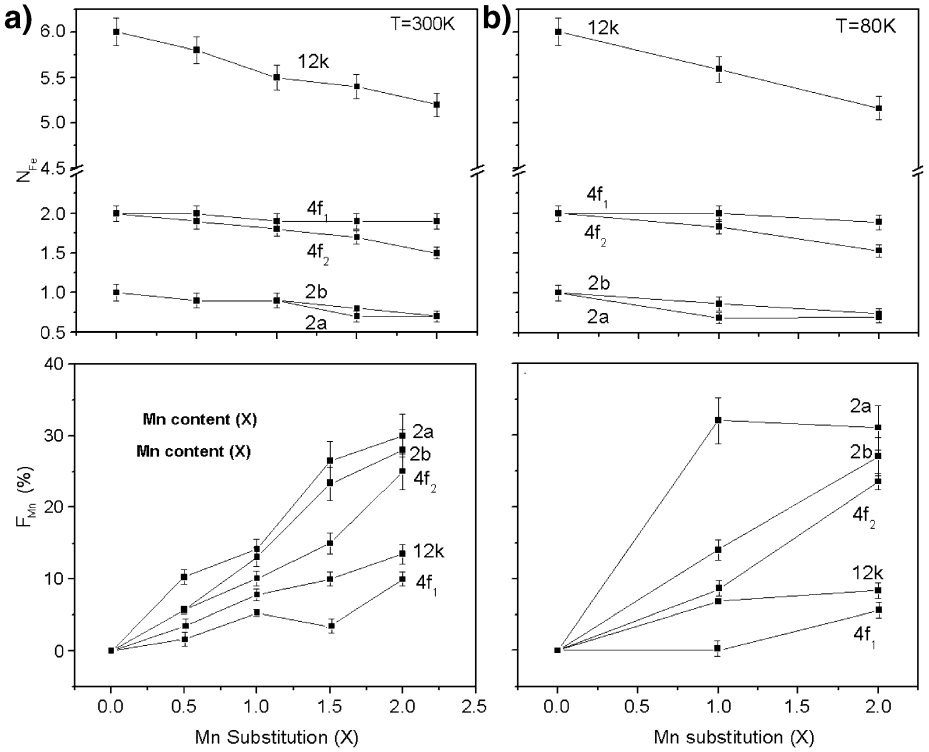

Fig. 4 Site occupation number for iron (N_{Fe}) and site occupation of Mn^{3+} ions on each site at 300 K (**a**) and 80 K (**b**)

In order to estimate the Mn^{3+} ion occupation, the site occupation numbers for iron ion, $N_{Fe,}$ and the associated Mn^{3+} ion occupancy fraction, F_{Mn}, were calculated by using the formulae [8]

$$N_{\mathrm{Fe}}(i) = C_{\mathrm{Fe}} \left[\frac{S(i)}{\sum_{i=1}^{5} S(i)} \right]$$

$$F_{Mn} = \frac{N(i) - N_{Fe}(i)}{N(i)} \times 100\%,$$

where C_{Fe} denotes the iron content (i.e., $C_{Fe}=12-X$), $S(i)$ is the subspectral area of the ith site obtained from the least square fit and $N(i)$ is the occupation number for the ith site.

It can be seen from the Fig. 4 (a and b), that Mn^{3+} ions occupy all the sites, although the $4f_1$ site is least substituted which is diverse to previously reported studies [12]. The site occupation numbers and the site occupation fractions, as obtained from the Mössbauer characterizations at RT and 80K, reveal satisfactory consistency, exception to the 2a site that, for $X=1.0$, shows an occupation fraction for $T=80$ K almost three times the value obtained for RT. In our opinion, this is much more a product of the limited resolution (i.e.,

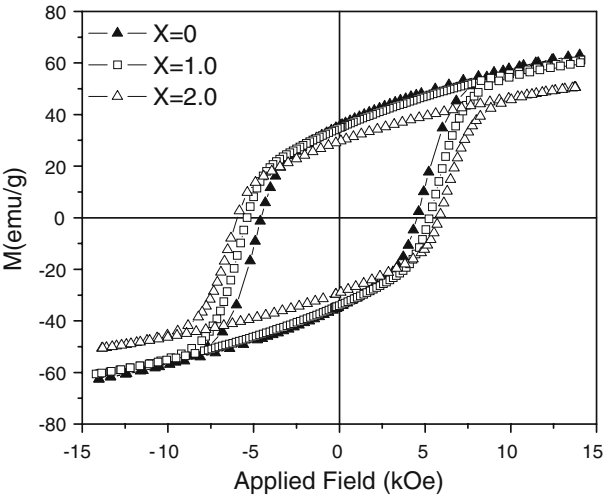

Fig. 5 RT magnetization curves, as a function of the applied field, for the $BaFe_{12}O_{19}$, $BaFe_{11}Mn_{1.0}O_{19}$ and $BaFe_{10}Mn_2O_{19}$ samples

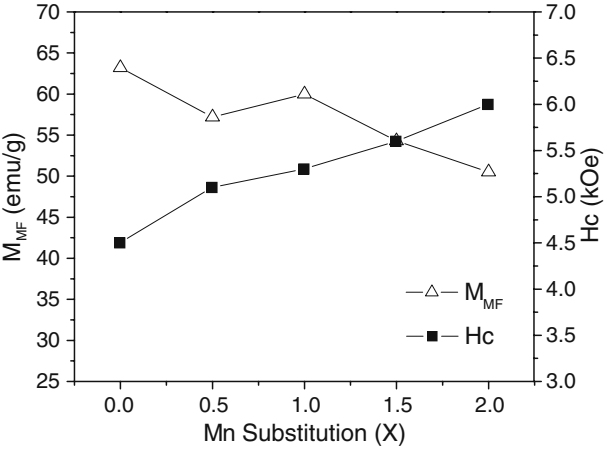

Fig. 6 Magnetization at maximum field and coercivity, as a function of Mn content, for the $BaFe_{12-X}Mn_XO_{19}$ samples

the uncertainty) of the fitted area parameters than a differentiated change with temperature in the f factors respective to the various iron sites in the hexaferrite structure.

Figure 5 shows the RT magnetization curves, as a function of the applied field, for the X= 0.0, 1.0 and 2.0 samples. A lower magnetization at maximum field, M_{MF}, and a higher coercivity are evident in the Mn-substituted samples.

The variation of M_{MF} with the Mn substitution is shown in the Fig. 6. The lower saturation magnetization could be understood by the site occupation of Mn^{3+} ions, which takes place for all the sites, spin up (12k, 2a, 2b) or spin down ($4f_1$, $4f_2$) sites. However, the percent site occupation in the spin up sites is quite higher as compared to the spin down sites. This higher level of occupation at spin up sites may result in a smaller magnetic moment decreasing, therefore, the M_{MF} in Mn-substituted samples.

Figure 6 also shows the variation of coercivity upon Mn substitution. The coercivity increases with the substitution amount. This may attributed to the decrease in the hexagonal

c axis, since the shrinkage would lower the Fe^{3+}–O–Fe^{3+} bond lengths, enhancing the superexchange interaction and, consequently, the coercivity. Our previous investigation revealed that lower substitution levels do not affect the lattice parameters. The observed increase in coercivity was mainly ascribed to the reduction in the grain size [15].

4 Conclusions

Mn-substituted barium hexaferrites were prepared by high-energy ball milling and subsequent heat treatment at 1050°C. It was observed from the Mössbauer investigation that Mn substitution above X=0.5 affects the 12k site, splitting it in two, $12k_1$ and $12k_2$. Both are further transformed to only one (12k) site at 80 K. The occupation number and occupancy fraction of Mn ion suggest that Mn^{3+} ion substituted all five crystallographic sites. The magnetization decreases with the substitution amount due to the dilution of the magnetic structure. The increase in coercivity is due to the decrease in lattice parameter, *c*, which may enhance the superexchange interaction between neighboring Fe^{3+} ions.

Acknowledgements The authors would like to thank to the Brazillian agencies, CNPq (Bolsa PDJ) and CAPES, for financial support.

References

1. Speliotis, D.E.: IEEE Trans. Magn. **23**, (5), 3143 (1987)
2. Kojima, H.: Ferromagnetic materials. In: Wohlfarth, E. P. (ed.), vol. 3, Chapter 5 (1982)
3. An, S.Y., Shim, I., Kim, C.S.: J. Appl. Phys. **91**, (10), 8465 (2002)
4. Zhou, X.Z., Morrish, H.: J. Appl. Phys. **75**, (10), 5556 (1994)
5. Turrili, G., Licci, F., Paoluzi, A., Besagni, T.: IEEE Trans. Magn. **24**, (4), 2146 (1987)
6. Wartewig, P., Krause, M.K., Esquinazi, P., Rösler, S., Sonntag, R.: J. Magn. Magn. Mater. **192**(1), 83 (1999)
7. Gonzalez-Angeles, A., Suarez, G.M., Gruskova, A., Papanova, M., Slama, J.: Mater. Lett. **59**, 26 (2005)
8. Li, Z.W., Ong, C.K., Yang, Z., Wei, F.W., Zhou, X.Z., Zhao, J.H., Morrish, A.H.: Phys. Rev. B **62**, (10), 6530 (2000)
9. Wang, S., Ding, J., Shi, Y., Chen, J.: J. Magn. Magn. Mater. **219**, 206 (2000)
10. Clark, T.M., Evans, B.J., Thompson, G.K.: J. Appl. Phys. **85**, (2), 5229 (1999)
11. Ounnunkad, S., Winotai, P.: J. Magn. Magn. Mater. **301**, (2), 292 (2006)
12. Collomb, A., Obradors, X., Isalgué, A., Fruchart, D.: J. Magn. Magn. Mater. **69**, 317 (1987)
13. Turilli, G., Licci, F., Rinaldi, S.: J. Magn. Magn. Mater. **59**, 127 (1986)
14. Schmid, H.K., Mader, W.: Micron. **37**, 426(2006)
15. Sharma, P., Rocha, R.A., Medeiros, S.N., Hallouche, B., Paesano Jr., A.: J. Magn. Magn. Mater. **316**, 29 (2007)